VNU Journal of Science: Natural Sciences and Technology
Journal homepage: https://js.vnu.edu.vn/NST

Original Article

Synthesis of Highly Fluorescent Nitrogen and Sulfur Co-Doped Carbon Quantum Dots Using Microwave-Assisted Method

Phạm Thị Ngọc Mai, Nguyễn Hoàng Minh, Trần Ngọc Bích, Trần Đông Dương, Vũ Duy Tùng, Chu Thị Huệ, Nguyễn Thị Kim Thường, Nguyễn Thị Ánh Hường, Phạm Gia Bách*

VNU University of Science, 19 Le Thanh Tong, Hoan Kiem, Hanoi, Vietnam

Received 14th April 2025
Revised 28th January 2026; Accepted 14th April 2026

Abstract: This study presents the synthesis of highly fluorescent nitrogen and sulfur co-doped carbon quantum dots (NS-CQDs) using a microwave-assisted method. Citric acid monohydrate and thiourea were used as precursors, and the synthesis was completed in just 7 minutes under microwave irradiation at 800W. The resulting NS-CQDs, with an average size of 5 to 8 nm, were characterized using X-ray diffraction (XRD), energy-dispersive X-ray spectroscopy (EDX), Fourier-transform infrared spectroscopy (FT-IR), transmission electron microscopy (TEM), and UV-Vis spectroscopy. These techniques confirmed the successful doping of nitrogen and sulfur into the carbon quantum dots, as well as the presence of various functional groups that enhance their hydrophilicity and chemical reactivity. The NS-CQDs exhibited strong absorption in the UV region and emitted bright blue fluorescence with a peak at 435 nm upon excitation at 365 nm, achieving a quantum yield of 26.9%. The fluorescence properties of NS-CQDs were found to be pH-sensitive, with maximum intensity observed at pH 7. Additionally, the NS-CQDs demonstrated excellent stability under UV irradiation and long-term storage. Due to their unique optical properties and stability, NS-CQDs hold significant potential for applications in biosensing, bioimaging, drug delivery, and optoelectronics.

Keywords: Carbon quantum dots; microwave assisted synthesis.

1. Introduction

Fluorescent sensors are attractive due to their notable characteristics such as affordability, ease of use, quick analysis, and high sensitivity. They have become the focus of attention for developing quantitative analytical techniques by utilizing changes in fluorescent intensity or emission peak position, either through enhancement or quenching [1, 2]. Unlike other semiconductor quantum dots, Carbon Quantum Dots (CQDs) present straightforward synthesis processes, efficient dispersal in water, remarkable photostability,

* Corresponding author.
E-mail address: phamgiabach@hus.edu.vn

https://doi.org/10.25073/2588-1140/vnunst.5836

non-toxicity, biocompatibility, and enhanced chemical stability [2, 3].

While traditional carbon quantum dots (CQDs) possess advantageous features, they suffer from limitations in fluorescence yield [4, 5]. To address this challenge, doping CQDs with heteroatoms has been shown to efficiently enhance their optical properties [6, 7]. Doping introduces new energy levels within the bandgap of CQDs, leading to enhanced and tunable optical properties [6]. Additionally, doping enhances the chemical reactivity and stability of CQDs, making them more robust for use in harsh environments or in applications requiring long-term stability [8]. Common elements for doping CQDs include nitrogen, sulfur, phosphorus, and boron.

Among various heteroatoms, nitrogen and sulfur dopants have garnered significant attention due to their wide range of precursors, natural abundance in sustainable sources, and cost-effective synthesis methods [9]. Nitrogen, with an atomic radius similar to carbon, and sulfur, with comparable electronegativity to carbon, make nitrogen and sulfur co-doped carbon quantum dots (N,S-CQDs) particularly noteworthy among doped CQDs. N-doped CQDs or nitrogen/sulfur co-doped CQDs (N,S-CQDs) exhibit significantly higher fluorescence quantum efficiency and photocatalytic activity compared to their undoped counterparts [10]. This enhanced performance makes N,S-CQDs valuable in applications such as biological imaging [11] and fluorescent sensing [12, 13] due to their high quantum yield.

One of the distinguishing features of N,S-CQDs is their ability to fine-tune optoelectronic properties through various synthetic methods, setting them apart from undoped CQDs [14]. This tuning introduces new energy states within the bandgap, facilitating radiative recombination, which in turn leads to a higher quantum yield and stronger emission intensity [15]. Nitrogen doping functionalizes the CQD surface with amino and pyrrolic groups, thereby improving solubility and biocompatibility-key factors for biological applications [16, 17]. Otherwise, sulfur doping in carbon quantum dots (CQDs) imparts additional advantageous properties, notably enhancing electrical conductivity [18], which makes these nanomaterials suitable for electronic applications. Moreover, sulfur-doped CQDs demonstrate improved stability against photobleaching and salt-induced aggregation [19], both critical for practical utilization. The incorporation of sulfur atoms also introduces functional groups such as thiols and sulfones to the CQD surface, providing versatile platforms for further chemical modifications and functionalization.

CQDs and N,S-CQDs are easy to synthesize from various carbon sources at a very low cost using either "top-down" or "bottom-up" approaches [20]. Among these two approach, bottom-up approaches, which involve the pyrolysis or carbonization of small organic molecules into larger structures to form CQDs, have advantages such as fewer defects and high controllability. The most widely used bottom-up methods are pyrolysis or carbonization, hydrothermal, solvothermal, and microwave-assisted methods. Pyrolysis produces CQDs with high quantum yields but requires long synthesis times (up to 48 hours). Hydrothermal and solvothermal methods are also widely used for synthesizing CQDs, but they require the precursor to be heated in a sealed autoclave at high temperatures [21]. Although the synthesis time is usually shorter, the quantum yield is not as high as with the pyrolysis method.

Microwave-assisted synthesis is a promising approach due to its rapid and uniform heating capabilities, resulting in shorter reaction times and higher yields compared to conventional methods [22]. This method also offers additional benefits, such as low operational cost, simplicity, and minimal byproduct formation. Consequently, microwave-assisted synthesis has been widely adopted in laboratories to produce CQDs with high reaction efficiency and satisfactory quantum yields [23-25]. Despite several studies reporting the microwave-assisted synthesis of

N,S-CQDs, the synthesis conditions-including microwave irradiation duration and power-vary considerably, resulting in quantum yields ranging from approximately 19% to 27%. To address this variability, our study focuses on optimizing the microwave-assisted synthesis protocol and thoroughly characterizing the resulting N,S-CQDs. The primary aim is to establish a robust, reproducible synthesis method and gain comprehensive insights into the surface characteristics and fluorescence behavior of these nanomaterials. Such advancements will significantly enhance the effectiveness and reliability of biosensors, expanding their potential in diverse analytical applications.

2. Experimental

2.1. Chemicals

All chemicals used in this research are analytical reagent grade purity (AR), including, citric acid monohydrate (Fisher, USA, ≥ 99,8% purity); thiourea (Sigma-Aldrich, USA, ≥ 99,0% purity); hydrochloric acid (Merck, Germany); Sodium hydroxide (Merck, Germany, ≥ 99,0% purity); acetonitrile (ACS, 99.5+%, Thermo Scientific Chemicals, USA) and deionized water.

2.2. Instruments

Fluorescence spectra were recorded on F-4700 (HITACHI, Japan) fluorescence spectrophotometer, using four transparent sides 1-cm path quartz cuvette, in the wavelength range from 380-600 nm, with excitation wavelength of 360 nm. UV-Vis spectra were recorded on UV-1601 (Shimadzu, Japan) spectrometer, using 1-cm path quartz cuvette. The morphology, structural properties and elemental composition of materials were characterized on FTIR-1S (Shimadzu, Japan), Transmission Electron Microscopy (TEM) (JEOL JEM 1010, Japan), Scanning Electron Microscopy (SEM) (JEOL JSM-IT200, Japan) with X-ray Dispersive Spectroscopy (EDS), and X-ray Diffraction (XRD) (Bruker D8 Advance, USA) using excitation source Cu Kα at λ = 1.54 Å. N,S-CQDs were synthesized on Toshiba MW3-MM25PE(BK) 25 L 800 W microwave. The zeta potential of the N,S-CQDs was determined using a Zetasizer Nano ZS (Malvern Instruments, Malvern, UK) in distilled water at solution pH values of 2.20, 5.00, and 8.00 to evaluate the surface charge characteristics of the nanoparticles. The centrifugation step was carried out using a Hettich EBA 200 centrifuge (Germany) at 6000 rpm for 15 minutes. Ultrasonication was performed using a WUC-D10H ultrasonic cleaner (Daihan Scientific, Korea) with a frequency of 40 kHz for 10 minutes. Dialysis was conducted using a cellulose membrane dialysis bag with a molecular weight cut-off (MWCO) of 1000 Da (Spectra/Por®, Repligen, USA) at room temperature (25 °C) for 24 hours.

2.3. Synthesis Route of CQDs, N,S-CQDs

N,S-CQDs were synthesized following a straightforward microwave-assisted protocol adapted from previous reports with slight modifications [23-25]. Briefly, 0.50 g of citric acid monohydrate and 0.50 g of thiourea were dissolved in 25 mL of deionized water. The homogeneous solution was placed in a conventional microwave and irradiated for 7 minutes at a power setting of 800 W, transforming into a black, viscous liquid, indicative of successful carbonization. Following carbonization, 25 mL of additional deionized water was added, and the mixture was ultrasonicated for 10 minutes to facilitate dispersion of the newly formed quantum dots. The resulting suspension was then centrifuged at 6000 rpm for 15 minutes and filtered through a 0.22 μm microfilter. To ensure complete removal of residual impurities, the filtrate was dialyzed for 24 hours at 25 °C. Finally, the purified N,S-CQDs solution was lyophilized to obtain a brown-black solid, which was stored for subsequent use. For comparative purposes, undoped CQDs were synthesized using 1.0 g of citric acid monohydrate under identical reaction and post-synthesis treatment conditions.

2.4. Calculation of Quantum Yield (QY)

The quantum yield of N,S-CQDs and CQDs is calculated by the following formula:

$$\Phi_S = \Phi_R \left(\frac{I_S}{I_R}\right)\left(\frac{A_R}{A_S}\right)\left(\frac{n_S}{n_R}\right)^2 \qquad (1)$$

where Φ is the fluorescence quantum yield (QY (%)), I is the integrated fluorescence intensity, A is the absorbance of the fluorophore, and n is the refractive index of the solvents (water, n = 1,33). the subscript 'R' refers to the fluorescence standard reference, quinine sulfate (quantum yield = 54.6%) in 0.1 M H_2SO_4, while the subscript 'S' refers to the sample (either N,S-CQDs or CQDs). All of the solutions' absorbance were kept below 0.1 a.u to avoid inner filter effect.

The absorbance of N,S-CQDs was measured at 365 nm, and their fluorescence intensity was recorded at 435 nm using an excitation wavelength of 365 nm. For undoped CQDs, absorbance was measured at 375 nm, while fluorescence intensity was measured at 460 nm with an excitation wavelength of 375 nm. Quinine in 0.1 M H_2SO_4, used as the reference, showed an absorbance peak at 350 nm and a fluorescence emission at 450 nm upon excitation at 350 nm.

3. Results and Discusions

3.1. Structural and Morphological Characterisation of N,S-CQDs

The crystal structure of N,S-CQDs was analyzed using X-ray diffraction (XRD). The XRD spectrum of N,S-CQDs (Figure 1a) reveals a broad peak at 23.5°, corresponding to the (002) diffraction planes in the CQDs. This peak is indicative of the carbonaceous core of the CQDs and aligns with previous studies, which report an interlayer spacing of the graphitic structure with a distance of 0.37 nm [26]. The Energy Dispersive X-ray (EDX) spectrum of N,S-CQDs (Figure 1b) displays strong characteristic peaks for the elements C (0.27 KeV), N (0.38 KeV), and O (0.52 KeV), along with a smaller peak for S (2.31 KeV). The overall composition of the N, S-CQDs from elemental analysis was C 62.72 wt%, O 17.82 wt%, N 10.11 wt%, and S 3.16 wt%.These findings confirm the successful incorporation of nitrogen and sulfur dopants into the N,S-CQDs structure.

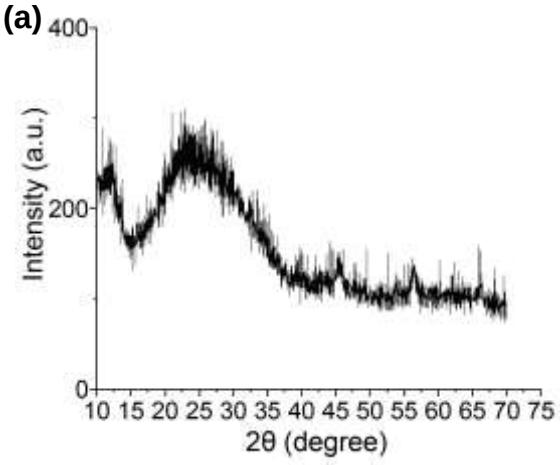

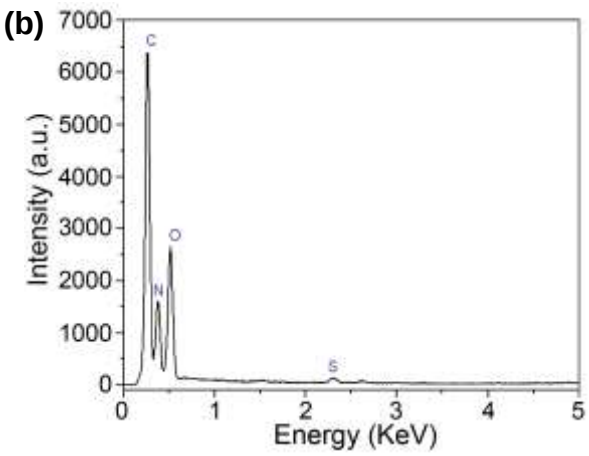

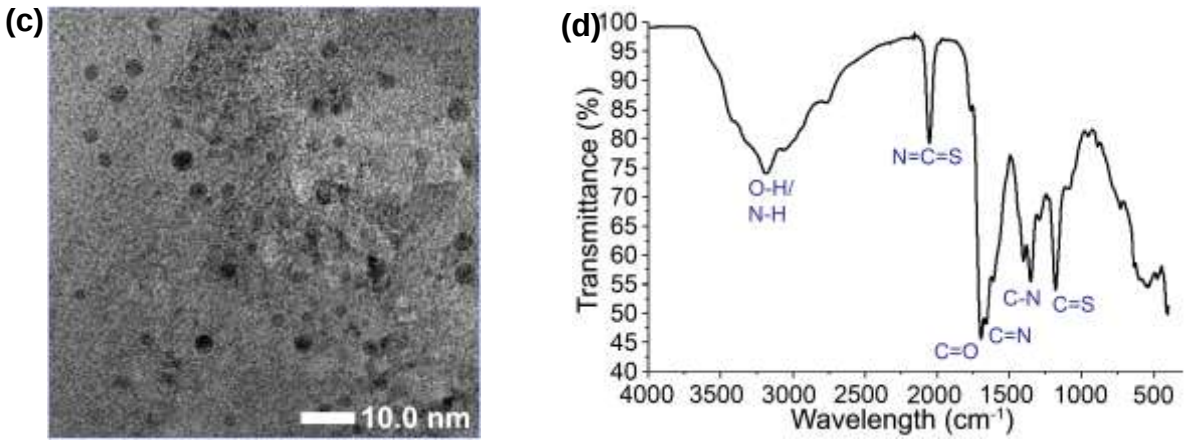

Figure 1. Characterisation of N,S-CQDs (a) XRD pattern;
(b) EDX spectrum (c) TEM image; (d) FT-IR spectrum.

The surface morphology of N,S-CQDs was examined using TEM analysis (Figure 1c). The TEM image reveals the presence of spherical dots with particle sizes ranging from 5 to 8 nm, indicating the successful synthesis of the nanomaterial through a simple and cost-effective procedure.

The infrared (IR) spectra of N,S-CQDs, covering the wavenumber range of 400-4000 cm^{-1} (Figure 1d). A broad band observed from 2800 cm^{-1} to 3400 cm^{-1} demonstrates the presence of O-H/N-H bonds, which contribute to the dispersion and hydrophilicity of N,S-CQDs in polar solvents. A sharp peak at 2054 cm^{-1} is attributed to the stretching of the thiocyanate group (N=C=S). The characteristic peaks at 1699 cm^{-1} and 1661 cm^{-1} are assigned to C=O and C=N groups of amides and imines/oximes, respectively. Additionally, a small absorption band at 1403 cm^{-1} indicates the presence of carboxyl functionalities on the surface of the CQDs. Peaks at 1354 cm^{-1} and 1180 cm^{-1} can be asigned to C-N and C=S bonds, respectively [9].

3.2. Surface Charge

The surface-charge characteristics of N,S-CQDs and CQDs were assessed by measuring their zeta potentials in three conditions: i) Immediately after synthesis (N,S-CQDs, pH 2.25; CQDs, pH 2.50); and ii) After adjusting separate aliquots to pH 5.00 and pH 8.00 by the dropwise addition of 0.1 M HCl or 0.1 M NaOH, respectively. The results (Table 1), indicate that the surface of N,S-CQDs is negatively charged, with increasing negativity as the pH rises. This trend can be explained by the deprotonation of carboxylic acid groups on the surface of the quantum dots at higher pH levels. As the pH rises above their typical pKa range (approximately 3 to 5), these groups lose protons and become negatively charged carboxylate ions ($–COO^–$), thereby increasing the overall negative surface charge. Additionally, N,S-CQDs exhibit a more pronounced negative surface charge compared to undoped CQDs, which can be attributed to the incorporation of sulfur-containing functional groups such as C=S and thiocyanate. These groups possess strong electron-withdrawing properties, leading to an increased density of negative charges on the nanoparticle surface. This observation is supported by FTIR analysis, which shows characteristic absorption bands corresponding to C=S and other sulfur-related functionalities.

Previous studies have shown that the zeta potential of carbon quantum dots (CQDs) can range from highly negative to highly positive, depending on their surface functional groups and the surrounding pH. CQDs bearing carboxyl or hydroxyl groups typically exhibit negative zeta potentials (e.g., −16 mV to −31.7 mV), whereas those containing amine groups can display positive zeta potentials (e.g., +36 mV) at neutral Ph [27]. It is generally accepted that colloidal stability is highest when the zeta potential exceeds ±30 mV, although the exact threshold can vary depending on the specific type of CQD and environmental conditions. In this study, the N,S-CQDs exhibited a persistently negative surface charge across a broad pH range, with a zeta potential more negative than −30 mV at pH 8.0. This strong and stable negative charge suggests that N,S-CQDs are well-suited for the detection of positively charged species, such as metal ions or cationic molecules, under various pH conditions [12].

Table 1. Zeta potential of N,S-CQDs and CQDs at different pH

Measured quantities	N,S-CQDs			CQDs		
	pH 2.25	pH 5.00	pH 8.00	pH 2.50	pH 5.00	pH 8.00
Mean Zeta potential (mV)	-6.69	-16.20	-31.53	0.8093	-12.32	-14.37
Conductivity (mS/cm)	1.27	2.22	3.76	1.118	0.59	1.13
Standard deviations (mV)	5.59	1.91	2.21	1.300	5.01	1.10

3.3. Spectrophotometric and Fluorescence Properties of N,S-CQDs

3.3.1. Molecular Absorption Spectra of N,S-CQDs

In addition to XRD, UV-Vis spectroscopy is employed to further characterize the synthesized material. Figure 2a shows the UV-Vis spectra of N,S-CQDs and undoped CQDs within the wavelength range of 200-700 nm. Both doped and undoped CQDs exhibit a strong absorption band in the 200-300 nm range, which is attributed to the π-π* transition of C=C bonds. Notably, the UV-Vis spectrum of N,S-CQDs displays a characteristic shoulder peak at 340 nm, which is less discernible in the spectrum of undoped CQDs. This difference arises from the n-π* transition of aromatic sp^2 C=N bonds in N,S-CQDs, which enhances absorption at this wavelength, in contrast to the C=O n-π* transition in undoped CQDs. These findings are consistent with previous studies [28, 29].

3.3.2. Fluorescence Ability of N,S-CQDs

The excitation-dependent emission properties of N,S-CQDs were analyzed to evaluate the stability of the synthesized particles. Measurements were conducted across an excitation wavelength range of 200 to 380 nm (Figure 2b). The fluorescence spectrum revealed a maximum emission intensity at 435 nm with an excitation wavelength of 365 nm. Notably, this indicates a red-shift in the excitation wavelength and a blue-shift in the emission wavelength compared to undoped CQDs (λ_{ex} = 375 nm, λ_{em} = 460 nm). A possible explanation for the observed blue-shift in the emission spectrum of our N,S-CQDs is an increase in the band gap energy, leading to higher-energy, shorter-wavelength fluorescence. Although N,S co-doping is often associated with the introduction of mid-gap

states that narrow the band gap and cause red-shifted emission, certain doping configurations-such as pyridinic nitrogen or smaller particle sizes-have been reported to enhance quantum confinement effects and potentially widen the band gap [8]. These structural or compositional variations could be contributing to the blue-shift observed in our study. However, the photoluminescence behavior of N,S-CQDs is known to be highly sensitive to synthesis conditions and dopant distribution, and thus, this explanation remains tentative. Further structural and spectroscopic investigations are necessary to confirm the underlying mechanism. Based on these findings, all subsequent fluorescence emission studies were performed with an excitation wavelength of 365 nm and an emission wavelength of 435 nm for N,S-CQDs.

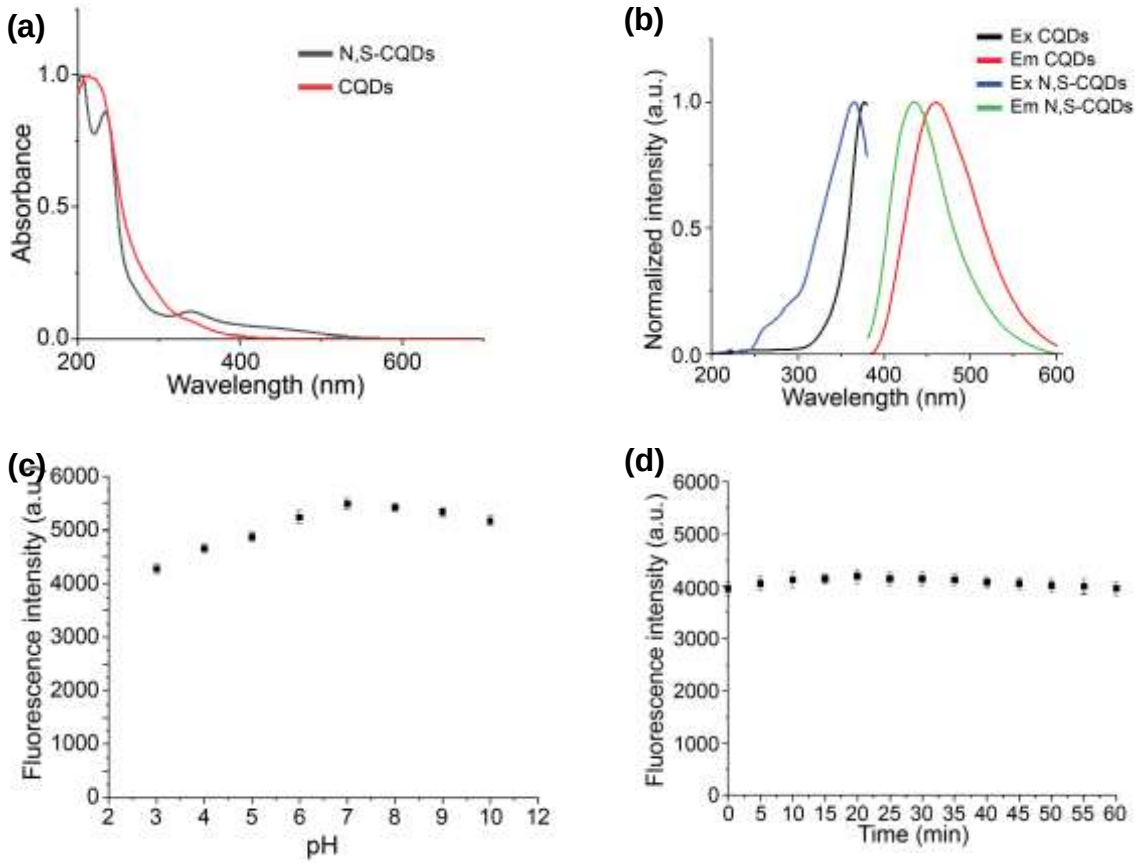

Figure 2. *(a)* UV-Vis spectra of N,S-CQDs and undoped CQDs;
(b) Fluorescence spectra of CQDs and N,S-CQDs;
(c) Effect of pH on fluorescence emission of N,S-CQDs;
(d) Stability of N,S-CQDs under continuous irradiation.

The fluorescent efficiency of a fluorophore is typically determined by its quantum yield, which is defined as the ratio of the number of photons emitted to the number of photons absorbed. A higher quantum yield indicates a more fluorescent material. To assess the fluorescent properties of N,S-CQDs and CQDs, quantum yield measurements were conducted using quinine sulfate in 0.1 M H_2SO_4 as a fluorescence standard reference. The quantum

yield standard curves for quinine sulfate, N,S-CQDs, and CQDs are presented in Table 2. The quantum yield of N,S-CQDs in solution was calculated to be 26.9%, which is higher than most reported values for microwave-assisted synthesis of CQDs and significantly higher than the quantum yield of undoped CQDs under the same conditions, which was measured at 15.7% [10].

3.3.3. The pH-dependent Fluorescence Emission Ability of N,S-CQDs Solution

The pH of the solution can significantly influence the fluorescence emission of N,S-CQDs (Figure 2c). The fluorescence intensity increases as the pH rises from 3.0 to 7.0, after which it decreases at higher pH levels. This pattern can be attributed to pH-dependent changes in the surface charge of N,S-CQDs, influenced by the protonation and deprotonation of functional groups such as carboxyl (–COOH) on their surface. At low pH, the –COOH groups are predominantly protonated, leading to a reduction in surface negative charge. This decreases the electrostatic repulsion between particles, promoting aggregation. As the pH increases, these functional groups become deprotonated, resulting in an increase in negative surface charge. The enhanced electrostatic repulsion among the negatively charged particles improves their colloidal stability and dispersion. However, at higher pH levels, the strongly negative surface may attract counterions such as Na^+, which can form a layer around the particles, screen the repulsive forces, and consequently induce aggregation [30]. Overall, the stability of N,S-CQDs across a moderate pH range suggests their suitability for applications in environments where pH may fluctuate, particularly between pH 6 and 9. Within this range, the fluorescence intensity remains relatively stable, with variations of less than 10%, indicating their potential for use in sensing and biological applications.

Table 2. Quantum yield calculations of N,S-CQDs and CQDs

Fluorophores	Solvent	Standard curve	R^2	QY (%)
Quinine sulfate	Water (n = 1.33)	I = 61381 A + 815.36	0.9997	54.6%
N,S-CQDs		I = 30196 A + 215.75	0.9987	26.9%
CQDs		I = 17643 A – 112.75	0.9878	15.7%

3.3.4. Stability of N,S-CQDs Solution

The stability of the N,S-CQDs solution was assessed by monitoring changes in fluorescence intensity under continuous irradiation (Figure 2d). Initially, the CQDs absorb photons and emit light, leading to a slight increase in fluorescence intensity. After 25 minutes, the fluorescence intensity gradually decreases, ranging from 0.50% to 1.16% after 60 minutes of irradiation. This indicates that N,S-CQDs exhibit good stability under UV light. Additionally, the N,S-CQDs solution remains stable for at least a month when stored at 4 °C in a tightly sealed, amber-colored container to prevent exposure to light and air. Under these storage conditions, the solution showed no signs of turbidity, precipitation, or decline in fluorescence intensity. This high stability, combined with their remarkably strong fluorescence, suggests that N,S-CQDs are promising candidates for applications as fluorescent nanosensors in analytical chemistry, as well as in other potential fields such as bioimaging, drug delivery, and optoelectronics.

4. Conclusion

This study successfully demonstrates a rapid and straightforward synthesis of nitrogen and sulfur co-doped carbon quantum dots (N,S-CQDs) using a microwave-assisted method. The synthesis was completed in under

10 minutes without the use of complex organic solvents, representing a significant improvement over conventional pyrolysis methods, which typically require synthesis times of up to 48 hours. Characterization techniques, including TEM, EDS, UV-Vis, and IR spectroscopy, confirmed that the synthesized N,S-CQDs possess a graphitic core capped with functional groups such as -COOH, -OH, -NH, and -SH, which confer high solubility in water and strong reactivity with organic compounds. The co-doping of nitrogen and sulfur significantly enhances the quantum yield of N,S-CQDs to 26.9%, compared to 15.7% for undoped CQDs, and also results in a more negatively charged surface. The N,S-CQDs exhibit strong blue fluorescence, excellent optical properties, and good fluorescence stability, along with notable pH sensitivity. These features, combined with their robust stability under UV irradiation and consistent performance over time, make N,S-CQDs particularly promising for a wide range of applications, including biosensing, bioimaging, drug delivery, and optoelectronic devices. Further research may focus on further exploring these potential applications and optimizing the synthesis process for large-scale production.

Acknowledgements

This research is conducted under Project QG.23.75 of Vietnam National University.

References

[1] H. Wang, S. Jiang, Z. Xu, L. Xu, A Novel Fluorescent Sensor Based on a Magnetic Covalent Organic Framework-Supported, Carbon Dot-Embedded Molecularly Imprinted Composite for the Specific Optosensing of Bisphenol a in Foods, Sensors and Actuators B: Chemical, Vol. 361, 2022, pp. 131729.

[2] Q. K. Nguyen, D. T. Nguyen, T. M. A. Pham, B. Pham, T. A. H. Nguyen, T. D. Pham et al., A Highly Sensitive Fluorescence Nanosensor for Determination of Amikacin Antibiotics Using Composites of Carbon Quantum Dots and Gold Nanoparticles, Spectrochimica Acta Part A: Molecular and Biomolecular Spectroscopy, Vol. 305, 2024, pp. 123466.

[3] F. Yuan, S. Li, Z. Fan, X. Meng, L. Fan, S. Yang, Shining Carbon Dots: Synthesis and Biomedical and Optoelectronic Applications, Nano Today, Vol. 11, No. 5, 2016, pp. 565-586.

[4] P. G. Luo, S. Sahu, S. T. Yang, S. K. Sonkar, J. Wang, H. Wang et al., Carbon "Quantum" Dots for Optical Bioimaging, Journal of Materials Chemistry B, Vol. 1, No. 16, 2013, pp. 2116-2127.

[5] L. Li, G. Wu, G. Yang, J. Peng, J. Zhao, J. J. Zhu, Focusing on Luminescent Graphene Quantum Dots: Current Status and Future Perspectives, Nanoscale, Vol. 5, No. 10, 2013, pp. 4015-4039.

[6] X. Kou, S. Jiang, S. J. Park, L. Y. Meng, A Review: Recent Advances in Preparations and Applications of Heteroatom-Doped Carbon Quantum Dots, Dalton Transactions, Vol. 49, No. 21, 2020, pp. 6915-6938.

[7] S. D. Dsouza, M. Buerkle, P. Brunet, C. Maddi, D. B. Padmanaban, A. Morelli et al., The Importance of Surface States in N-Doped Carbon Quantum Dots, Carbon, Vol. 183, 2021, pp. 1-11.

[8] H. Lu, C. Li, H. Wang, X. Wang, S. Xu, Biomass-Derived Sulfur, Nitrogen Co-Doped Carbon Dots for Colorimetric and Fluorescent Dual Mode Detection of Silver (I) and Cell Imaging, ACS Omega, Vol. 4, No. 25, 2019, pp. 21500-21508.

[9] Y. W. Zeng, D. K. Ma, W. Wang, J. J. Chen, L. Zhou, Y. Z. Zheng et al., N, S Co-Doped Carbon Dots with Orange Luminescence Synthesized through Polymerization and Carbonization Reaction of Amino Acids, Applied Surface Science, Vol. 342, 2015, pp. 136-143.

[10] S. Yang, X. Sun, Z. Wang, X. Wang, G. Guo, Q. Pu, Anomalous Enhancement of Fluorescence of Carbon Dots through Lanthanum Doping and Potential Application in Intracellular Imaging of Ferric Ion, Nano Research, Vol. 11, 2018, pp. 1369-1378.

[11] R. K. Das, S. Panda, C. S. Bhol, S. K. Bhutia, S. Mohapatra, N-Doped Carbon Quantum Dot (NCQD)-Deposited Carbon Capsules for Synergistic Fluorescence Imaging and Photothermal Therapy of Oral Cancer, Langmuir, Vol. 35, No. 47, 2019, pp. 15320-15329.

[12] H. Wu, C. Tong, Nitrogen- and Sulfur-Codoped Carbon Dots for Highly Selective and Sensitive Fluorescent Detection of Hg2+ Ions and Sulfide in Environmental Water Samples, Journal of Agricultural and Food Chemistry, Vol. 67, No. 10, 2019, pp. 2794-2800.

[13] Y. Li, Y. Hu, Y. Jia, X. Jiang, Z. Cheng, N, S Co-Doped Carbon Quantum Dots for the Selective and Sensitive Fluorescent Determination of

N-Acetyl-L-Cysteine in Pharmaceutical Products and Urine, Analytical Letters, Vol. 52, No. 11, 2019, pp. 1711-1731.

[14] S. A. Shaik, S. Sengupta, R. S. Varma, M. B. Gawande, A. Goswami, Syntheses of N-Doped Carbon Quantum Dots (NCQDs) from Bioderived Precursors: A Timely Update, ACS Sustainable Chemistry & Engineering, Vol. 9, No. 1, 2020, pp. 3-49.

[15] J. Tang, J. Zhang, Y. Zhang, Y. Xiao, Y. Shi, Y. Chen et al., Influence of Group Modification at the Edges of Carbon Quantum Dots on Fluorescent Emission, Nanoscale Research Letters, Vol. 14, 2019, pp. 1-10.

[16] Y. Guo, W. Zhao, Hydrothermal Synthesis of Highly Fluorescent Nitrogen-Doped Carbon Quantum Dots with Good Biocompatibility and the Application for Sensing Ellagic Acid, Spectrochimica Acta Part A: Molecular and Biomolecular Spectroscopy, Vol. 240, 2020, pp. 118580.

[17] S. Chandra, D. Bano, P. Pradhan, V. K. Singh, P. K. Yadav, D. Sinha et al., Nitrogen/Sulfur-Co-Doped Carbon Quantum Dots: A Biocompatible Material for the Selective Detection of Picric Acid in Aqueous Solution and Living Cells, Analytical and Bioanalytical Chemistry, Vol. 412, 2020, pp. 3753-3763.

[18] K. W. Sung, K. Y. Ko, H. J. Ahn, Tailored Sulfur and Nitrogen Co-Doped Carbon Quantum Dot Interfacial Layer on Copper Foil for Highly Stable and Ultrafast Lithium-Ion Capacitors, Journal of Energy Storage, Vol. 72, 2023, pp. 108797.

[19] J. R. Adsetts, S. Hoesterey, C. Gao, D. A. Love, Z. Ding, Electrochemiluminescence and Photoluminescence of Carbon Quantum Dots Controlled by Aggregation-Induced Emission, Aggregation-Caused Quenching, and Interfacial Reactions, Langmuir, Vol. 36, No. 47, 2020, pp. 14432–14442.

[20] R. Wang, K. Q. Lu, Z. R. Tang, Y. J. Xu, Recent Progress in Carbon Quantum Dots: Synthesis, Properties and Applications in Photocatalysis, Journal of Materials Chemistry A, Vol. 5, No. 8, 2017, pp. 3717-3734.

[21] A. Mozdbar, A. Nouralishahi, S. Fatemi, G. Mirakhori, eds., The Effect of Precursor on the Optical Properties of Carbon Quantum Dots Synthesized by Hydrothermal/Solvothermal Method, AIP Conference Proceedings, AIP Publishing, 2018.

[22] Y. Pang, H. Gao, S. Wu, X. Li, Facile Synthesis the Nitrogen and Sulfur Co-Doped Carbon Dots for Selective Fluorescence Detection of Heavy Metal Ions, Materials Letters, Vol. 193, 2017, pp. 236-239.

[23] K. K. Chan, C. Yang, Y. H. Chien, N. Panwar, K. T. Yong, A Facile Synthesis of Label-Free Carbon Dots with Unique Selectivity-Tunable Characteristics for Ferric Ion Detection and Cellular Imaging Applications, New Journal of Chemistry, Vol. 43, No. 12, 2019, pp. 4734-4744.

[24] R. Tabaraki, N. Sadeghinejad, Microwave Assisted Synthesis of Doped Carbon Dots and Their Application as Green and Simple Turn Off–On Fluorescent Sensor for Mercury (II) and Iodide in Environmental Samples, Ecotoxicology and Environmental Safety, Vol. 153, 2018, pp. 101-106.

[25] M. P. Szmyt, B. Buszewski, R. G. Kopciuch, Sulphur and Nitrogen Doped Carbon Dots Synthesis by Microwave Assisted Method as Quantitative Analytical Nano-Tool for Mercury Ion Sensing, Materials Chemistry and Physics, Vol. 242, 2020, pp. 122484.

[26] Z. Qin, W. Wang, X. Zhan, X. Du, Q. Zhang, R. Zhang et al., One-Pot Synthesis of Dual Carbon Dots Using Only an N and S Co-Existed Dopant for Fluorescence Detection of Ag+, Spectrochimica Acta Part A: Molecular and Biomolecular Spectroscopy, Vol. 208, 2019, pp. 162-171.

[27] J. S. Boruah, K. Sankaranarayanan, D. Chowdhury, Insight into Carbon Quantum Dot–Vesicles Interactions: Role of Functional Groups, RSC Advances, Vol. 12, No. 7, 2022, pp. 4382-4394.

[28] G. Magdy, N. Said, R. A. E. Domany, F. Belal, Nitrogen and Sulfur-Doped Carbon Quantum Dots as Fluorescent Nanoprobes for Spectrofluorimetric Determination of Olanzapine and Diazepam in Biological Fluids and Dosage Forms: Application to Content Uniformity Testing, BMC Chemistry, Vol. 16, No. 1, 2022, pp. 98.

[29] S. R. Kamali, C. N. Chen, D. C. Agrawal, T. H. Wei, Sulfur-Doped Carbon Dots Synthesis under Microwave Irradiation as Turn-Off Fluorescent Sensor for Cr (III), Journal of Analytical Science and Technology, Vol. 12, 2021, pp. 1-11.

[30] Q. Li, B. Chen, B. Xing, Aggregation Kinetics and Self-Assembly Mechanisms of Graphene Quantum Dots in Aqueous Solutions: Cooperative Effects of pH and Electrolytes, Environmental Science & Technology, Vol. 51, No. 3, 2017, pp. 1364-1376.